Local inhibition of ornithine decarboxylase reduces vascular stenosis in a murine model of carotid injury

Forte, Amalia; Grossi, Mario; Turczynska, Karolina; Svedberg, Kaj; Rinaldi, Barbara; Donniacuo, Maria; Holm, Anders; Baldetorp, Bo; Vicchio, Mariano; De Feo, Marisa; Sante, Pasquale; Galderisi, Umberto; Berrino, Liberato; Rossi, Francesco; Hellstrand, Per; Nilsson, Bengt-Olof; Cipollaro, Marilena

Published in:
International Journal of Cardiology

DOI:
10.1016/j.ijcard.2013.04.153

2013

Local inhibition of ornithine decarboxylase reduces vascular stenosis in a murine model of carotid injury

*#1Amalia Forte, #1,4Mario Grossi, 4Karolina M. Turczynska, 4Kaj Svedberg, 1Barbara Rinaldi, 1Maria Donniacuo, 4Anders Holm, 5Bo Baldetorp, 3Mariano Vicchio, 2Marisa De Feo, 2Pasquale Santè, 1Umberto Galderisi, 1Liberato Berrino, 1Francesco Rossi, 4Per Hellstrand, 4Bengt-Olof Nilsson, 1Marilena Cipollaro

Dept. of 1Experimental Medicine, 2Cardiothoracic and Respiratory Sciences, 3Anesthesiological, Surgical and Emergency Sciences, 1,2Excellence Research Centre for Cardiovascular Diseases, Second University of Naples, Italy; Dept. of 4Experimental Medical Science, 5Clinical Science, Lund University, Sweden

1, 2, 3, 4, 5: This author takes responsibility for all aspects of the reliability and freedom from bias of the data presented and their discussed interpretation.

***Correspondence to:**

Prof. Marilena Cipollaro

Department of Experimental Medicine

Second University of Naples

Via L. De Crecchio, 7- 80138 Naples, Italy

E-mail: marilena.cipollaro @unina2.it

Phone: ++39-081-5665879

Fax ++39-081-5667547

#: Contributed equally to this study.

ABSTRACT

Objectives: Polyamines are organic polycations playing an essential role in cell proliferation and differentiation, as well as in cell contractility, migration and apoptosis. These processes are known to contribute to restenosis, a pathophysiological process often occurring in patients submitted to revascularization procedures. We aimed to test the effect of α-difluoromethylornithine (DFMO), an inhibitor of ornithine decarboxylase, on vascular cell pathophysiology *in vitro* and in a rat model of carotid arteriotomy-induced (re)stenosis.

Methods: The effect of DFMO on primary rat smooth muscle cells (SMCs) and mouse microvascular bEnd.3 endothelial cells (ECs) was evaluated through the analysis of DNA synthesis, polyamine concentration, cell viability, cell cycle phase distribution and by RT-PCR targeting cyclins and genes belonging to the polyamine pathway. The effect of DFMO was then evaluated in arteriotomy-injured rat carotids through the analysis of cell proliferation and apoptosis, RT-PCR and immunohistochemical analysis of differential gene expression.

Results: DFMO showed a differential effect on SMCs and on ECs, with a marked, sustained anti-proliferative effect of DFMO at 3 and 8 days of treatment on SMCs and a less pronounced, late effect on bEnd.3 ECs at 8 days of DFMO treatment. DFMO applied perivascularly in pluronic gel at arteriotomy site reduced subsequent cell proliferation and preserved smooth muscle differentiation without affecting the endothelial coverage. Lumen area in DFMO-treated carotids was 49% greater than in control arteries 4 weeks after injury.

Conclusions: Our data support the key role of polyamines in restenosis and suggest a novel therapeutic approach for this pathophysiological process.

Abstract word count: 250

Key words: restenosis, negative remodelling, ornithine decarboxylase, α-difluoromethylornithine, endothelial cells, smooth muscle cells.

1. Introduction

The polyamines spermidine and spermine, and their precursor putrescine, are positively charged molecules expressed by all living organisms and known to play an essential role in cell proliferation and differentiation. They are also involved in cell contractility and migration as well as in apoptosis. All these processes are known to contribute to restenosis after revascularization procedures, a pathophysiological process that is reduced but not eliminated by the advent of bare metal stents and of drug-eluting stents [1].

Several studies have highlighted the multiplicity of mechanisms and levels of action of polyamines in influencing cell functions in healthy and pathological settings. For example, polyamines can modulate the functions of DNA, nucleotide triphosphates and proteins. In particular, polyamines can stabilize the double-stranded DNA by increasing the melting temperature, and can promote DNA bending, thus influencing the recognition of regulatory proteins by their response elements and contributing to regulation of gene transcription [2]. Polyamines can also modulate the functions of RNA and most of them exist in a polyamine-RNA complex in cells [3], revealing their ability to regulate gene expression also post-transcriptionally. Interestingly, polyamines seem to play a role also in epithelial-to-mesenchymal transition (EMT), a phenomenon linked to cell plasticity that could have a pivotal function in tissue remodelling [4].

Considering the multiplicity of phenomena in which polyamines are involved, they could play a key role in restenosis progression, as well as to show a potential as therapeutic targets to prevent or reduce this recurrent pathophysiological phenomenon. Indirect evidence for a role of polyamines in stenosis progression has come from preclinical models of vascular injury [5-8]. These findings further supported a role for growth- and migration-stimulatory polyamines in stenosis progression. Despite this premise, the experimental inhibition of polyamine synthesis and/or uptake has been poorly investigated in animal models of vascular disease, as only a few studies so far have focused on the interference with polyamine biosynthesis in restenosis [9, 10].

In this study we aimed to analyse the potential therapeutic role of a local perivascular application of α-difluoromethylornithine (DFMO), an irreversible inhibitor of ornithine decarboxylase (ODC), in a model of surgically-induced rat carotid (re)stenosis. ODC is the first rate-limiting enzyme in the polyamine anabolic pathway, catalyzing the conversion of ornithine into putrescine, and as such playing a key role in polyamine biosynthesis [3].

The *in vivo* experiments have been supported and integrated by a panel of *in vitro* assays performed on rat primary carotid smooth muscle cells (SMCs) and on mouse bEnd.3 endothelial cells (ECs) to examine the influence of DFMO on cell physiology, including possible tissue-specific differences.

2. Methods

2.1 Cells and cell culture

The mouse microvascular EC line bEnd.3 was purchased from American Type Tissue Culture Collection (Manassas, VA, USA). Primary rat carotid SMCs were isolated from male Sprague Dawley rats (250–300 g) euthanized by CO_2 as approved by the regional Animal Ethics Committee, Lund and Malmö. Left and right common carotid arteries were removed and dissected free of surrounding tissue under sterile conditions. Subsequently the vessels were incubated for 30 min at 37ºC in serum free Dulbeccos Modified Eagle's Medium (DMEM) containing 1 mg/ml collagenase type 2 (Worthington Biochemical Corporation, Lakewood, NJ, USA). The adventitia was then pulled off using forceps and the carotid arteries were incubated for 3-4 h at 37ºC in serum free DMEM cell culture media containing 2 mg/ml collagenase type 2 and 0.1 mg/ml elastase (Sigma). The primary SMCs were seeded, allowed to divide and trypsinized (0.25%) upon reaching confluence. The primary rat carotid SMCs were used for experiments in passages 2-4. The bEnd.3 ECs and primary rat carotid SMCs were cultured in a mixture (1:1) of DMEM and Ham's F12 medium with addition of antibiotics (50 U/ml penicillin and 50 µg/ml streptomycin) and 10% fetal calf serum.

All experiments were performed in sub-confluent (~ 70% confluence) cells. Prior to experiments the cells were made quiescent by culturing with serum-free media for 24 h. The cells were pre-incubated with DFMO for 2 h before they were growth-stimulated with 5% fetal calf serum for 3 and 8 days in the continued presence or absence of DFMO. DFMO was kindly provided by Hoechst Marion Roussel, Cincinnati, OH, USA and dissolved in phosphate buffered saline (PBS).

2.2 Determination of polyamine concentration

The polyamines were determined in cellular homogenate by HPLC and normalized to total protein as described by Seiler and Knodgen [11]. Cellular polyamine concentration was expressed as nmol/mg total protein.

2.3 Immunocytochemistry

Cultured cells were grown on glass cover slips for immunocytochemistry. Cells were fixed in 4% paraformaldehyde for 10 min at room temperature, washed carefully in PBS and then mounted on microscope slides. SM α-actin immunoreactivity was determined using a mouse monoclonal antibody (clone 1-A4, Sigma) at 1:200 dilution. SM22α immunoreactivity was assessed using a rabbit polyclonal antibody (Abcam, Cambridge, UK) at 1:200 dilution. Microtubule structure was assessed using a mouse monoclonal α-tubulin antibody (clone B-5-1-2, Sigma) at 1:4000 dilution. Immunofluorescence was visualized using a Cy3-conjugated secondary anti-mouse or a Cy5-conjugated secondary anti-rabbit antibody at 1:500 dilution (Invitrogen, Carlsbad, CA, USA). The glass cover slips with cells stained for the respective primary and secondary antibody were carefully washed. The nuclei were counterstained with Sytox green (Invitrogen). Fluorescence was analyzed using laser-scanning confocal microscopy (LSM 5 Pascal, Carl Zeiss AG, Göttingen, Germany).

2.4 Determination of DNA synthesis

DNA synthesis was determined by measuring incorporation of radio-labelled methyl-[^{3}H]-thymidine (PerkinElmer Inc., Boston, MA, USA) into newly synthesized DNA. The isotope (5 μCi) was included for the last hour of the 3-8 days incubation with DFMO. The cells were washed in PBS, harvested using a rubber policeman, and sonicated in 5 mM NaOH twice for 10 s. Aliquots of the sonicate were precipitated with 5% trichloroacetic acid and centrifuged (10000 g for 2 min at 4˚C). After washing with 5% trichloroacetic acid, the pellet was dissolved in Soluene. Liquid scintillation cocktail was added and the radioactivity measured in a liquid scintillation counter (Beckman, Fullerton, CA, USA). Radioactivity was expressed as disintegrations per minute (D.P.M.) and normalised to total protein concentration in each sample, determined using a Bio-Rad protein assay kit (Bio-Rad, Hercules, CA, USA) based on the Lowry method [12].

2.5 Cell counting and cell viability

The number of cells was determined by counting the trypsinized (0.25% trypsin) cells in a Bürker chamber. The trypan blue exclusion test was used to analyze cell viability. Cell culture medium was removed, cells washed with 0.9% NaCl and then cells were incubated for 2 min with 0.4% trypan blue (Sigma). Thereafter, the cells were washed 3 times in 0.9% NaCl. The number of cells containing trypan blue was determined as a measure of dead/dying cells.

2.6 Determination of cell cycle phase distribution by flow cytometry

Distribution of cells in the cell cycle was analyzed by flow cytometry of propidium iodide-stained nuclei at 3 days in DFMO treated and control cells as described by Odenlund et al. [13]. Briefly, flow cytometric DNA analysis was performed in a FACSCalibur flow cytometer (Becton Dickinson Immunocytometry Systems; San José; CA, USA). DNA contents were analyzed in about 13000 nuclei in each sample. Cell cycle phase distribution was determined using ModFit LT 3:1 (Verity Software House Inc., Topsham, ME, USA).

2.7 Animals

Studies were carried out on 12 week-old male Wistar rats (230-250 g) (Charles River, France). Rats were maintained in accordance with the guidelines of the NIH (Guide for the Care and Use of Laboratory Animals, 1976). All protocols were approved by the Animal Care and Use Committee of the Second University of Naples. Rats were acclimatized and quarantined for at least one week before undergoing surgery.

2.8 Vascular Injury and DFMO treatment

Rats were anesthetized with i.p. injection of 100 mg/kg ketamine and 0.25 mg/kg medetomidine and carefully placed onto a warm surface and positioned for surgery. All the surgical procedures were conducted with sterile techniques and vital signs were continuously monitored through a

pulsioxymeter. Arteriotomy of rat common carotid artery was performed as already published [14]. Briefly, a plastic Scanlom clamp for coronary artery grafting was placed for 10 seconds on the carotid causing a crushing lesion to the vessel. At the same point where the clamp was applied, a 0.5 mm longitudinal incision was done on the full thickness of the carotid. The incision did not cross to the other side of the vessel. Haemostasis was obtained with a single adventitial 8.0-gauge polypropylene stitch. Once bleeding stopped, the carotid artery was carefully examined and blood pulsation was checked distally to the incision. Rats were administered 100 μl of 5 mg/mL DFMO in 20% pluronic gel F127 (Sigma) perivascularly applied to the arteriotomy-injured carotid. Control rats were administered 100 μl of 20% pluronic gel only. Pluronic poloxamer gel is hydrofilic and is liquid at 4°C but rapidly solidifies when in contact with tissues at 37°C. After gelification, the skin was approximated by a reabsorbable suture. Animals were allowed to wake up through an intramuscular injection of 1 mg/kg atipamezol. Postoperative systemic analgesia was administered through subcutaneous injection of 0.1 mg/kg buprenorphine every 8 hours. Antibiotics therapy was administered through subcutaneous injection of 5 mg/kg enrofloxacin once a day for 3 days following the arteriotomy procedure.

2.9 RNA extraction and RT-PCR analysis

Total RNA was extracted from injured rat carotids at 3 hrs and at 3 days after arteriotomy (n=5 DFMO-treated rats and n=5 pluronic gel-treated rats, for each time point), from uninjured rat carotids (n=4) and from primary rat SMCs and mouse bEnd.3 cells (n=3 for each group, for each time point) using the RNAeasy minikit (Qiagen) according to manufacturer's instructions. RT-PCR experiments were performed as already published [15]. GeneBank sequences for rat mRNAs and the Primer Express software (Applied Biosystem) were used to design primer pairs for the genes belonging to the polyamine metabolism and to the other pathways we selected as of interest in our model. Primer sequences are reported in Supplemental Table 1.

2.10 Immunohistochemistry

Hybridisations were performed on carotid arteries taken at 3 days after arteriotomy and DFMO or pluronic gel perivascular application and on control carotids taken from uninjured rats after anesthesia (n=8 for each group). Carotid cross-sections were dewaxed, rehydrated with descending concentrations of ethanol and rinsed in distilled water. Antigen retrieval was performed by microwaving. Sections were stained with a polyclonal rabbit SM22α antibody (Sigma Chemicals, St. Louis, MO, USA) at 1:500 dilution and with a polyclonal rabbit Von Willebrand Factor (vWF) antibody (DAKO A/S, Glostrup, Denmark) at 1:100 dilution. Fluorescence was analyzed by laser-scanning confocal microscopy using the Zeiss Pascal and custom-written software.

2.11 BrdU proliferation assay

Rats were submitted to carotid arteriotomy and to DFMO or pluronic gel perivascular application. Eighteen hrs prior to sacrifice at 3 days after injury (n=8 for each group) they were administered 50 mg/kg bromodeoxyuridine (BrdU) (Roche Applied Science) i.p. for detection and quantification of cells that entered into the cell cycle within 18 hrs of sacrifice. The 4% formaldehyde-fixed sections (5 μm) were deparaffinized and rehydrated. Immunohistochemical detection of incorporated BrdU was performed through a primary antibody anti-BrdU (Roche Applied Science, monoclonal anti-mouse, 6 μg/mL) as previously published [15]. Image screening and photography of serial cross-sections submitted to colorimetric immunohistochemical analysis were performed using a Leica IM1000 System. Five cross-sections localized at the injury site were analyzed for each carotid. The percentages of BrdU-positive nuclei in the tunicae intima and media were calculated by determining the number of hematoxylin-stained nuclei in the tunicae intima and media positive for immunohistochemical staining of BrdU. A number of randomly selected slides were quantified for BrdU staining by two independent observers blinded to the rat treatment to assess inter-observer variation.

2.12 TUNEL assay

Assays were performed on carotid arteries taken at 3 days after arteriotomy and DFMO or pluronic gel perivascular application and on control carotids taken from uninjured rats after anesthesia (n=8 for each group). The 4% formaldehyde-fixed sections (5 μm) were deparaffinized and rehydrated. Immunohistochemical detection of fragmented DNA in apoptotic cells was performed through the In situ Cell Death Detection Kit, POD (Roche Applied Science) as previously published [15]. Specimen image screening and photography were performed using a Leica F4000 System. Five cross-sections localized at the injury site were analyzed for each carotid. The percentages of apoptotic nuclei in the tunicae intima and media were calculated by determining the number of hematoxylin-stained nuclei positive for TUNEL staining. When observed with 40-100x objectives, cells showing morphological features typically associated with apoptosis, as well as positive to TUNEL reaction, were considered to be apoptotic. A number of randomly selected slides were quantified for TUNEL staining by two independent observers blinded to rat treatment to assess inter-observer variation.

2.13 Morphometric analysis

Carotid arteries were harvested at 3 (n= 5 for each group), 7 (n=5 for each group) and 28 (n=10 for each group) days after arteriotomy and DFMO or pluronic gel application for morphological and morphometric analysis. Harvested vessels were fixed in 4% buffered formaldehyde, dehydrated and embedded in paraffin. Five micrometers cross-sections were stained with hematoxylin. Image screening and photography of serial cross-sections were performed using a Leica IM1000 System. Lumen cross-sectional area (CSA) was measured using the Leica IM1000 software. The lumen CSA of each injured carotid at the arteriotomy site was compared both to the ipsilateral distal region and to contralateral uninjured carotid. Measurements were performed by two independent observers.

2.14 Enzyme-linked Immunoadsorbent Assay (ELISA)

The concentration of Vascular endothelial growth factor (Vegf) in serum samples taken at 3 hrs and 3 days after arteriotomy from rats submitted to perivascular DFMO or pluronic gel application (n=5 for each group) and from uninjured rats (n=3) was measured using commercial ELISA kits (R&D Systems, code RRV00, minimum detectable dose of Vegf <0.09 pg/mL) following the manufacturer's instructions. Optical density was measured at 450 nm using an ELISA plate reader (Bio-Rad).

2.15 Statistical analysis

Summarized data are presented as means ± SEM. Statistical significance was calculated using the Student's two-tailed t test for unpaired comparison or the two-way analysis of variance followed by Bonferroni's multiple comparison test through the GraphPad software (San Diego, CA, USA) as appropriate. P-values < 0.05 were considered significant.

3. Results

3.1 DFMO reduces polyamines in cultured vascular smooth muscle and endothelial cells

In order to investigate the effects of DFMO on polyamine levels in vascular SMCs and ECs, the putrescine, spermidine and spermine concentrations were analyzed by HPLC. Treatment with 1 mM DFMO for 3 days completely eliminated putrescine and reduced spermidine by 87% and 72% in primary rat carotid SMCs and bEnd.3 ECs, respectively (Supplemental Table 2). Spermine concentration was unaffected by DFMO treatment in both cell types (Supplemental Table 2).

3.2 DFMO reduces vascular smooth muscle and endothelial cell DNA synthesis and cell number in a cell type-specific and time-dependent manner

The primary rat carotid SMCs showed characteristic "hill-and-valley" growth pattern and expressed the smooth muscle markers SM22α and smooth muscle α-actin, as shown in Fig. 1 A, B.

Cell proliferation was assessed by measuring cell number and DNA synthesis. DFMO (5 mM) reduced the number of SMCs but not that of ECs already at 3 days of treatment (Fig. 1C, D). Treatment with DFMO (1 and 5 mM) for 8 days reduced the cell number in both bEnd.3 ECs and primary rat carotid SMCs (Fig. 1C, D). Treatment with DFMO (1 and 5 mM) for 3 days had no effect on DNA synthesis in bEnd.3 ECs, while 5 mM DFMO reduced DNA synthesis in primary rat carotid SMCs by about 75% (Fig. 1E). 5 mM DFMO for 8 days resulted in an even more powerful inhibitory effect (90%) in SMCs and reduced DNA synthesis in bEnd.3 cells by about 30% (Fig. 1E). These data suggest that vascular SMCs respond earlier than ECs to DFMO growth inhibition.

No or very few trypan-blue positive ECs and SMCs were observed after treatment with 1 and 5 mM DFMO for 3 and 8 days (data not shown).

3.3 DFMO affects the cell cycle distribution of vascular smooth muscle and endothelial cells

The distribution of bEnd.3 and primary rat carotid SMCs in the cell cycle was analyzed by flow cytometry of propidium iodide-stained nuclei. Treatment with 5 mM DFMO for 3 days reduced the

number of primary rat carotid SMCs in S phase and increased the cell number in G_0/G_1 phase, suggesting that DFMO attenuates transition of the SMCs from G_0/G_1 into S (Fig. 1F). DFMO reduced the number of bEnd.3 ECs in the S phase and accumulated cells not only in the G_0/G_1 phase, but also in the G_2 phase of the cell cycle (Fig. 1F). The cell cycle phase distribution in ECs was more even than that in SMCs, irrespective of DFMO treatment (Fig. 1F). In consistency with the flow cytometry data, RT-PCR analysis of cyclins B1, D1 and E1 revealed a significant decrease of the mRNAs coding for cyclins B1 (71%) and E1 (86%) in primary vascular SMCs while a decrease of cyclin E1 only (30%) was observed in bEnd.3 ECs (Fig. 1L).

The immunoreactive signal of the von Willebrand factor (vWF) EC marker was unaffected by 3 days of treatment with DFMO in bEnd.3 ECs, but on the other hand the mRNA for vWF was slightly lowered (23%) by DFMO 1 day after DFMO treatment (data not shown). In order to investigate whether DFMO is able to affect cell proliferation by acting on polymerisation or depolymerisation of microtubules, we assessed the immunocytochemical staining for α-tubulin in bEnd.3 ECs treated with DFMO in comparison with control untreated ECs. As demonstrated in figure 1 G-I, the treatment with DFMO (1 and 5 mM) for 3 days had no effect on the structure of the bEnd.3 EC microtubule cytoskeleton.

3.4 DFMO affects the expression of genes involved in differentiation, signal transduction and proliferation in arteriotomy-injured carotids

We extracted total RNA from injured carotids harvested at 3 hrs and at 3 days after arteriotomy and DFMO (n=5 for each time point) or pluronic gel treatment (n=5 for each time point) and from carotids of uninjured rats (n=4). We analysed through RT-PCR the differential expression of the genes coding for interleukin 1b (Il1β), the monocyte chemoattractant protein-1 (Mcp1/Ccl2), the transforming growth factor beta 1 (Tgfb1) and its receptors I and II (Tgfbr1 and Tgfbr2), the vascular endothelial growth factor A (Vegfa) and its receptors Flt-1 and Flk-1, c-myc, the fibronectin (Fn) isoform ED-A Fn, the contractile SMC markers SM22α (Tagln), myocardin

(Myocd) and smoothelin (Smtn), the EC marker vWF and the transient receptor potential canonical cation channel proteins 1 and 6 (Trpc1 and Trpc6). These genes were chosen since they code for important proteins involved in inflammation as well as vascular growth, proliferation and differentiation, key processes in remodelling and restenosis. The expression data obtained in injured carotids were compared with the basal expression levels in carotids from uninjured rats.

The genes coding for markers of the SMC contractile phenotype (Tagln, Smtn) showed reduced expression both at 3 hrs and at 3 days (Tagln, Smn), whereas the transcriptional coactivator Myocd was decreased only at 3 days after arteriotomy in comparison with uninjured carotids ($p<0.05$). Comparison between control (pluronic-treated) and DFMO-treated arteries showed a significantly higher expression of all the three genes in DFMO-treated arteries at 3 days after arteriotomy (Fig. 2). A 50% decrease in vWF mRNA occurred in arteriotomy-injured carotids at 3 days after injury and, surprisingly, vWF mRNA was undetectable in DFMO-treated carotids at this time point (Fig. 2). Similar results were obtained in cultured bEnd.3 ECs, where DFMO treatment induced a significant decrease of vWF mRNA after 1 day of treatment (data not shown). The expression of SM22α and vWF was investigated also by immunostaining with confocal microscopy in arteriotomy-injured carotids at 3 days after arteriotomy and pluronic gel or DFMO treatment (n=8 for each group). While the expression analysis of SM22α confirmed the trend revealed by RT-PCR, with a significantly higher expression level in DFMO-treated than in control carotids (Fig. 3A-C), the vWF level, expressed as pixel intensity/length of the endothelium, did not differ between the two experimental groups either at the injury site (Fig. 3D-F) or at the distal region (data not shown), thus demonstrating the presence of a comparable endothelial layer in control and in DFMO-treated carotids.

The mRNAs coding for the Vegf receptors Flt-1 and Flk-1 showed a significantly lower expression in DFMO-treated carotids at 3 days after arteriotomy than in both injured and uninjured control carotids (Fig. 2). The expression of Vegf mRNA was unaffected by arteriotomy and by DFMO treatment (data not shown); nonetheless, the serum concentration of this growth factor increased

both at 3 hrs and 3 days after arteriotomy, and its increase was fully prevented by DFMO treatment ($p<0.05$) (Supplemental Fig. 1).

The expression of the cytokines Il1β and Mcp1 was activated by arteriotomy and increased by DFMO treatment at 3 hrs after arteriotomy (Fig. 2). As expected, the arteriotomy caused increase in Myc (3 h) and fibronectin (3 days) expression, indicating a proliferative response and matrix remodelling. However, none of these responses was affected by DFMO at the mRNA level. Although Tgfβr2 was slightly but significantly reduced by DFMO (Fig. 2), there was no effect on Tgfβ or Tgfβr1 expression (data not shown). The non-selective ion channels Trpc1 and Trpc6, which have been implicated in injury-induced smooth muscle phenotype modulation, were unaffected at mRNA level by DFMO treatment (data not shown).

3.5 DFMO affects the expression of genes belonging to the polyamine pathway in vitro and in arteriotomy-injured carotids

The expression profile of genes belonging to the polyamine pathway was evaluated in bEnd.3 ECs and in primary vascular SMCs at 3 days after 5mM DFMO treatment and in control untreated cells. We analysed the differential expression of genes coding for anabolic enzymes (ornithine decarboxylase 1-Odc1, arginase 1-Arg1, Arg2, adenosylmethionine decarboxylase 1-Amd1, spermidine synthase-Srm, spermine synthase-Sms) and catabolic enzymes (spermidine/spermine N1-acetyl transferase 1-Sat1, spermine oxidase-Smox, antizyme inhibitor 1-Azin1, ornithine decarboxylase antizyme 1-Oaz1, Oaz2) of the polyamine pathway.

All the genes were significantly affected by DFMO treatment in bEnd.3 cells, with the exception of Srm (Fig. 4). In particular, we observed a significant increased expression of two genes involved in polyamine synthesis (Odc1, Amd1) and a decrease of all other anabolic or catabolic enzymes ($p<0.05$). The effect of DFMO in primary SMCs were less pronounced, as it altered the expression of only 3 polyamine-related genes, inducing an increased expression of the mRNAs coding for the

anabolic enzymes Amd1 and Sms and a decrease of the mRNA coding for the catabolic enzyme Sat1 in comparison to control untreated cells (Fig. 4).

Surprisingly, the Smox mRNA was not expressed in primary SMCs, while, as expected, Arg2 was expressed exclusively in SMCs, as only some EC lines express this enzyme isoform [16, 17].

A parallel analysis of the *in vivo* expression profile of genes belonging to the polyamine pathway was performed on RNA extracted from carotids at 3 hrs and 3 days after arteriotomy with perivascular application of DFMO or pluronic gel only. Overall data indicate an alteration of the expression profile of genes belonging to the polyamine pathway in the acute phase following carotid arteriotomy, with a significant 1.9-fold increase of Odc1 at 3 hrs after injury and the activation of Arg1 expression both at 3 hrs and at 3 days after arteriotomy (Fig. 4). Srm levels were unaffected by arteriotomy and by DFMO treatment in comparison to basal levels measured in uninjured carotids. Other genes, including Smox, Sms, Arg2, Amd, Azin, Oaz1, Oaz2 and Sat1, showed a decrease below basal levels at 3 hrs and/or at 3 days after arteriotomy, often prevented (Arg1, Arg2, Oaz1, Oaz2, Sat1) or augmented (Smox) by DFMO treatment, respectively ($p<0.05$) (Fig. 4).

3.6 DFMO treatment affects cell proliferation index but not apoptosis after arteriotomy

We evaluated the effect *in vivo* of DFMO treatment on cell proliferation stimulated by arteriotomy giving a pulse of BrdU to rats subjected to carotid arteriotomy. Carotids were harvested at 3 days after arteriotomy and from uninjured rats and the cross sections at the injury site were submitted to BrdU immunohistochemical detection for assessment of the cell proliferation index. We considered for quantitative analysis positive cells located in the endothelium and in the media, as the adventitia was difficult to distinguish from perivascular tissue in injured carotids. Arteriotomy stimulated cell proliferation in carotids, with a mean 8.6% cells in the media and in the endothelium positive to BrdU incorporation at 3 days after arteriotomy (Fig. 5C-E), while no BrdU-positive cells were detectable in carotids from uninjured rats (Fig. 5E). The perivascular application of 5 mg/mL

DFMO after carotid arteriotomy induced a significant decrease to 4.5% of proliferating cells after arteriotomy ($p<0.05$) (Fig. 5A, B).

Carotid cross-sections adjacent to those used for BrdU proliferation assay were used to evaluate the apoptotic index at 3 days after arteriotomy and to verify the potential effect of the perivascular application of DFMO. At 3 days after arteriotomy we observed about 17% TUNEL-positive cells in the media and in the endothelium of injured carotids, in comparison to a basal 0.8% apoptotic cells in uninjured carotids (Fig. 5F, G, I). The local application of 5 mg/mL DFMO did not affect the percentage of apoptotic cells (Fig. 5I). These data were confirmed by the RT-PCR differential analysis of the anti-apoptotic gene Bcl-2 and of the pro-apoptotic gene Bax in carotids at 3 days after arteriotomy and DFMO or pluronic gel application, compared to uninjured carotids. Data showed a significantly decreased expression of Bcl-2 in all the samples we analysed after arteriotomy, irrespective of their treatment, while Bax expression showed a slight but significant decrease in DFMO-treated carotids (Fig. 5H). As a results, the Bcl-2/Bax ratio showed on average a 65% decrease in all the arteriotomy-injured carotids, supporting the activation of the apoptotic pathway by arteriotomy, irrespective of DFMO treatment.

3.7 Perivascular application of DFMO reduces rat carotid lumen stenosis 4 weeks after arteriotomy

Rat common carotids were submitted to arteriotomy and 5 mg/mL DFMO (n=20) or pluronic gel only (n=20) were locally applied at the injury site. The morphological and morphometric analysis of injured carotids was performed at 3 (n=5 for each group), 7 (n=5 for each group) and 28 days (n=10 for each group) after arteriotomy and treatment with DFMO or pluronic gel. Each carotid was compared to its contralateral uninjured artery (Fig. 6A) and to the distal ipsilateral uninjured region. Qualitative morphological analysis at 4 weeks after arteriotomy revealed that the injury induced a marked neoadventitia formation along with extracellular matrix and elastic lamina accumulation in

both groups of rats, with only limited focal neointima in a few cases (Fig. 6B, C). In addition, internal and external elastic lamina and media disruptions at the injury site were evident, often with media replacement by fibrotic tissue. Morphometric analysis showed a gradual decrease of lumen CSA at 7 and 28 days after arteriotomy in control injured carotids, while it remained substantially unaltered in DFMO-treated carotids, showing a significant 49% larger carotid lumen CSA in comparison to control pluronic gel-treated carotids 4 weeks after arteriotomy ($p<0.05$) (Fig. 6D). No significant difference in lumen CSA was evident between the distal regions of injured carotids belonging to the two experimental groups (data not shown).

4. Discussion

4.1 ODC inhibition triggers cell-type specific alterations in vitro

A major finding of our study is that primary rat carotid SMCs and bEnd.3 ECs showed differential reactions to DFMO with respect to cell cycle progression, DNA synthesis and cell number, despite the comparable decrease in spermidine concentration and the full putrescine depletion observed in both cell types. This suggests that DFMO can affect cell proliferation through diverse mechanisms, e.g. through different cyclins, depending on cell type. The RT-PCR differential analysis of mRNAs coding for cyclins B1, D1 and E1 confirmed this hypothesis. Cyclin E, in conjunction with CDK2, is known to trigger the S phase of the cell cycle, while the cyclin B-CDK1 complex is responsible for mitosis [18]. The impressive decrease of cyclin E in SMCs (86%), together with the slight but significant decrease of this cyclin also in ECs (30%), is in agreement with the arrest in the G_0/G_1 observed in both cell lines treated with DFMO. The significant decrease of cyclin B1 observed in SMCs only, suggests a role of DFMO in primary SMC progression towards mitosis.

Cell cycle data were supported by the DNA synthesis results and by the total number of living cells at 3 and 8 days after DFMO treatment, showing an earlier and significantly greater effect in primary SMCs than in bEnd.3 ECs. The overall data obtained in primary SMCs confirm that DFMO inhibits SMC proliferation in agreement with previous studies on cultured SMCs [19].

Consistency of our *in vitro* data relies on the fact that both the cell types we used, the primary rat SMCs and the bEnd.3 ECs, are representative of native vascular cells *in vivo*. The primary rat SMCs were shown to express smooth muscle α-actin and SM22α and the bEnd.3 ECs possess the typical EC morphology and express not only the EC markers eNOS and vWF [20], but also the classical estrogen receptor subtypes ERα and ERβ and the G-protein-coupled estrogen receptor 1 (GPER1) [21], confirming the expression patterns observed in ECs *in vivo*.

Finally, while some well-known anti-cancer drugs like taxol, vincristine and vinblastine, act by causing disruption of either polymerisation or depolymerisation of microtubules [22], our

immunocytochemical analysis of α-tubulin in bEnd.3 ECs suggests that DFMO exerts its antiproliferative effect through mechanisms distinct from the disruption of microtubules.

4.2 DFMO administration reduces polyamines in cultured cells and affects the expression of genes belonging to the polyamine pathway both in vitro and in vivo

Our data highlight the specificity of action of DFMO not only through the decrease or the depletion of intracellular polyamines *in vitro* but also through the alteration, both *in vitro* and *in vivo*, of the expression levels of genes belonging to the polyamine pathway, as a reaction to polyamine depletion caused by DFMO treatment in a pathophysiological setting where polyamines are dramatically required for cell proliferation. The decrease or depletion of putrescine and spermidine in the presence of DFMO, associated with other inhibitory results obtained for cell cycle, DNA synthesis and cell number, suggest that these two polyamines are important for the regulation of cell cycle progression and proliferation of SMCs.

The increased expression of genes involved in polyamine biosynthesis observed in injured carotids at 3hrs and/or at 3 days after arteriotomy is in agreement with previous findings [6, 10, 23]. Intracellular polyamine synthesis provides a primary polyamine source, supplying the cell with the adequate amounts of polyamines necessary for cell growth and proliferation [24, 25]. ODC is rapidly induced when the cell needs polyamines and therefore a high steady-state concentration of DFMO is necessary in close proximity to the proliferating cells, in order to prevent polyamine biosynthesis and cellular proliferation. In this study, we successfully achieved this through the local perivascular application of DFMO dissolved in pluronic gel, assuring a high local concentration of DFMO and minimizing potential systemic side effects.

Both cultured SMCs and ECs and the arteriotomy-injured carotids showed a trend for increased expression of polyamine anabolic enzymes and decreased expression of polyamine catabolic enzymes in the presence of DFMO. This was not sufficient to restore polyamine homeostasis as revealed by the *in vitro* data on primary SMCs and by the morphometric data obtained *in vivo* 4

weeks after arteriotomy. Nonetheless, significant differences emerge between primary SMCs and bEnd.3 ECs with respect to the differential expression of polyamine metabolism genes (Fig. 4). In general, RT-PCR data suggest that bEnd.3 ECs and SMCs could have a different efficiency of compensatory reactions to polyamine depletion induced by DFMO, which could be responsible for the differences in cell cycle phase distribution and in DNA synthesis.

The similar decrease or depletion we observed for polyamine concentration in the two cell types does not exclude differences possibly emerging at other time points following the DFMO treatment. Additional experiments should be done to specifically address this issue.

4.3 DFMO affects gene expression in arteriotomy-injured carotids

DFMO treatment induced differential effects on vWF mRNA and protein in arteriotomy-injured carotids and *in vitro*. The expression of vWF is tightly regulated and subject to post-translational modification [26], which may account for the different responses to DFMO at the mRNA and protein levels found here. Polyamines, due to their cationic charge, are able to interact with nucleic acids and to regulate gene transcription, but they are also able to regulate mRNA stability at a post-transcriptional level. Of interest, DFMO treatment of Rat-2 cells induced differential effects on mRNA expression, as some genes were down-regulated, while the expression of most genes was up-regulated [27]. The decrease of vWF mRNA following the DFMO-mediated polyamine depletion both *in vivo* and *in vitro* suggests decreased vWF mRNA stability and/or reduced transcription rate when polyamines are depleted, rather than deendothelialization induced by the arteriotomy, as also evidenced the immunohistochemical analysis. A similar mechanism could be proposed for mRNAs coding for the two Vegf receptors and for Tgfbr2, whose expression decreased below the basal levels in DFMO-treated carotids at 3 days after arteriotomy. Additional experiments will be necessary to verify a link between polyamine depletion and the reduction of transcription/stability of selected mRNAs.

Vegf is known to stimulate the proliferation of ECs and the migration and proliferation of SMCs [28]. Here we confirmed an increased serum concentration of this growth factor after arteriotomy [29]. Of interest, the local polyamine depletion at 3 hrs and at 3 days after arteriotomy prevented the increase of Vegf serum concentration in addition to its direct effects in the injured area.

Polyamines are endowed with an intrinsic anti-inflammatory activity, being able to down-regulate production of cytokines by macrophages [30], to mediate the effect of anti-inflammatory glucocorticoids and possibly to induce apoptosis of immune cells [31]. The increased expression of Il1β in DFMO treated carotids seems to confirm the link between polyamines and inflammation also in our model of vascular injury and could represent a potential limitation of the therapeutic strategy based on polyamine depletion. Additional studies will be necessary in this context.

The members of Tgfb family we analysed, together with the ED-A Fn isoform, are known to play a key role in vascular remodelling, mainly through the activation of myofibroblasts as a reaction to vascular injury [32]. Our RT-PCR data highlight a relevant increase of ED-A Fn and of Tgfb expression after arteriotomy, suggesting the activation of myofibroblast differentiation [6]. Nonetheless, this process does not appear to be affected by polyamine depletion, at least at transcriptional level.

The overall analysis of RT-PCR data obtained in arteriotomy-injured carotids indicates that the perivascular application of DFMO is effective in reducing intravascular polyamine concentrations already at 3 hrs following the vascular injury, as reflected by the early significant alterations of genes belonging to the polyamine metabolic pathway or involved in other pathophysiological phenomena.

4.4 DFMO does not affect the apoptotic index at 3 days after arteriotomy

The *in vivo* data did not demonstrate any significant effect on apoptosis stimulated by carotid arteriotomy at 3 days after injury. The role of polyamines in cell apoptosis is quite controversial, as different studies have led to opposite conclusions. Some recent studies support a pro-apoptotic

effect of polyamines mediated by an early induction of ODC and prevented by DFMO [33-35]. Other studies revealed that ODC inhibition reduces apoptosis [36], while some studies are in agreement with our findings of no effect on apoptosis [13]. The absence of signs of decreased cell viability due to DFMO we observed *in vitro* (data not shown) confirms the *in vivo* data and is also in agreement with previous observations showing that DFMO has a cytostatic rather than a cytotoxic effect [13, 37].

4.5 Perivascular application of DFMO reduces rat carotid lumen stenosis at 4 weeks after arteriotomy

There are currently only a few studies concerning the interference with polyamine biosynthesis in animal models of (re)stenosis. Endean et al. [9] inhibited the ODC activity in rabbits submitted to carotid deendothelization through the administration of 2% DFMO in drinking water, leading to a significant reduction of intimal hyperplasia at 2 and 4 weeks after injury. The authors claimed that these data resulted from the inhibition of an early burst of ODC activity following vascular injury. The key role of Arg1 in the remodelling response after arterial injury and hence its interest as an attractive therapeutic target has been highlighted in a study conducted in a rat carotid balloon angioplasty experimental model [10].

This study has been conducted in a rat pre-clinical model of vascular stenosis induced by arteriotomy, rather than by the classically applied balloon angioplasty. The arteriotomy model we set up mimics the damage that affects the arteries submitted to endarterectomy or to by-pass interposition, as it is based on a longitudinal incision of the vascular wall through its full thickness, including the internal and the external elastic laminae, sutured with a polypropilene stitch. This model of vascular injury has been applied in several studies to dissect both the molecular mechanisms triggered by arteriotomy, and to test potential therapeutic strategies [29, 38, 39].

Our morphometric results demonstrate that a limitation of the first wave of cell proliferation can effectively reduce the long-term restenosis, as suggested also by other studies in which a similar strategy has been successfully applied through other classes of inhibitory molecules [38, 40-42]. Of note, our strategy was able to overcome potentially increased uptake of circulating polyamines that could compensate for the decreased anabolism in arteriotomy-injured carotids through DFMO application. Thrombin is a serine protease known to be implicated in the pathogenesis of restenosis that is able to induce not only ODC expression in SMCs, but also the cationic amino acid transporters (CAT) 1 and 2, responsible for cellular uptake of L-ornithine [43]. An increased uptake of circulating polyamines also in our model of carotid arteriotomy is conceivable, as supported by our previous microarray-based studies revealing a 6-fold increased expression of CAT-1 in arteriotomy-injured carotids 4 hrs after injury [6]. However the potentially increased uptake was ineffective to overcome the inhibition of the synthesis of endogenous polyamines through the perivascular application of DFMO.

Of interest, carotid treatment with DFMO, blocking the polyamine biosynthesis, increases also the amount of L-arginine available for NO formation and furthermore NO itself has been suggested to inhibit ODC [44]. Thus, treatment with polyamine synthesis blockers, such as DFMO, inhibits polyamine formation and cell proliferation via a direct mechanism but probably also via an indirect mechanism involving elevated NO formation, able to inhibit ODC.

Previous studies demonstrated that DFMO is rapidly excreted from the body [45]. Consequently, high doses of DFMO are necessary to obtain a prolonged and effective inhibition of ODC. Moreover, DFMO should be immediately available at high concentration for a sufficient period of time after vascular injury as its target, the ODC enzyme, has a very short half-life (about 10 min-1 h in mammalian systems) and is readily destroyed by 26S proteasome [46, 47]. On the basis of DFMO and ODC characteristics, the local application of DFMO could potentially prove successful in reducing restenosis induced by vascular injury. This route of administration could allow high concentration of this drug in the acute phase after injury, when vascular cells (including SMCs,

fibroblasts, progenitor cells of various origin and myofibroblasts) are induced to proliferate to repair the injury. Pluronic gel F127 has been previously demonstrated not to affect vascular remodelling [48]. This copolymer works as a rate-controlling barrier and serves as a vehicle for the sustained release of drugs. It has been demonstrated that over a period of 3 hrs pluronic gel F127 releases 5.5% of the original dose of a drug at a gel concentration of 20-25%, or 3.8% of the original dose at a gel concentration of 30% [49]. Additional studies revealed that the drug release from pluronic gel is dependent solely on the gel concentration and on its dissolution rate, rather than on drug diffusion [50].

5. Conclusions

This study demonstrates a cell type-specific action of DFMO, with more pronounced antiproliferative effects on SMCs than on ECs. Overall results obtained *in vivo* confirmed the *in vitro* data and indicated that the local perivascular treatment of injured rat carotids with DFMO is effective in reducing arterial stenosis, mainly through a reduction of cell proliferation and of vessel remodelling, without affecting carotid endothelial coverage. These data highlight the therapeutic potential of a strategy based on locally applied DFMO, shedding a new light on this long-studied drug. DFMO might represent a new interesting drug-eluting stent concept, selectively reducing SMC proliferation in restenosis with very low toxicity. Additional experiments will be necessary to confirm the data in other pre-clinical models of vascular (re)stenosis and to further dissect the mechanisms of action of DFMO both on SMCs and on ECs.

Acknowledgements

This study was supported by grants from the Swedish Research Council, the Greta and Johan Kocks Foundation and the Thuréus Foundation.

We acknowledge the excellent technical assistance of Ina Nordström, M. Rosaria Cipollaro, Paolo Pariante and Lena Thiman. We are also grateful to Dr. Monica Mattia for excellent care of animal welfare.

The authors of this manuscript have certified that they comply with the Principles of Ethical Publishing in the International Journal of Cardiology [51].

Disclosures

None.

REFERENCES

[1] Song HG, Park DW, Kim YH, et al. Randomized trial of optimal treatment strategies for in-stent restenosis after drug-eluting stent implantation. J Am Coll Cardiol 2012;59:1093-100.

[2] Thomas T, Thomas TJ. Polyamines in cell growth and cell death: molecular mechanisms and therapeutic applications. Cell Mol Life Sci 2001;58:244-58.

[3] Igarashi K, Kashiwagi K. Modulation of cellular function by polyamines. Int J Biochem Cell Biol 2010;42:39-51.

[4] Prunotto M, Compagnone A, Bruschi M, et al. Endocellular polyamine availability modulates epithelial-to-mesenchymal transition and unfolded protein response in MDCK cells. Lab Invest 2010;90:929-39.

[5] Li JM, Zhang X, Nelson PR, et al. Temporal evolution of gene expression in rat carotid artery following balloon angioplasty. J Cell Biochem 2007;101:399-410.

[6] Forte A, Finicelli M, De Luca P, et al. Expression profiles in surgically-induced carotid stenosis: a combined transcriptomic and proteomic investigation. J Cell Mol Med 2008;12:1956-73.

[7] Nishida K, Abiko T, Ishihara M, Tomikawa M. Arterial injury-induced smooth muscle cell proliferation in rats is accompanied by increase in polyamine synthesis and level. Atherosclerosis 1990;83:119-25.

[8] Forte A, Hellstrand P, Nilsson BO, Grossi M, Rossi F, Cipollaro M. The polyamine pathway as a potential target for vascular diseases: focus on restenosis. Curr Vasc Pharmacol 2011;9:706-14.

[9] Endean ED, Kispert JF, Martin KW, O'Connor W. Intimal hyperplasia is reduced by ornithine decarboxylase inhibition. J Surg Res 1991;50:634-7.

[10] Peyton KJ, Ensenat D, Azam MA, et al. Arginase promotes neointima formation in rat injured carotid arteries. Arterioscler Thromb Vasc Biol 2009;29:488-94.

[11] Seiler N, Knodgen B. High-performance liquid chromatographic procedure for the simultaneous determination of the natural polyamines and their monoacetyl derivatives. J Chromatogr 1980;221:227-35.

[12] Lowry OH, Rosebrough NJ, Farr AL, Randall RJ. Protein measurement with the Folin phenol reagent. J Biol Chem 1951;193:265-75.

[13] Odenlund M, Holmqvist B, Baldetorp B, Hellstrand P, Nilsson BO. Polyamine synthesis inhibition induces S phase cell cycle arrest in vascular smooth muscle cells. Amino Acids 2009;36:273-82.

[14] Forte A, Di Micco G, Galderisi U, et al. Molecular analysis of arterial stenosis in rat carotids. J Cell Physiol 2001;186:307-13.

[15] Forte A, Finicelli M, Grossi M, et al. DNA damage and repair in a model of rat vascular injury. Clin Sci (Lond) 2009;

[16] Marinova GV, Loyaga-Rendon RY, Obayashi S, et al. Possible involvement of altered arginase activity, arginase type I and type II expressions, and nitric oxide production in occurrence of intimal hyperplasia in premenopausal human uterine arteries. J Pharmacol Sci 2008;106:385-93.

[17] Bachetti T, Comini L, Francolini G, et al. Arginase pathway in human endothelial cells in pathophysiological conditions. J Mol Cell Cardiol 2004;37:515-23.

[18] Bardin AJ, Amon A. Men and sin: what's the difference? Nat Rev Mol Cell Biol 2001;2:815-26.

[19] Thyberg J, Fredholm BB. Induction of ornithine decarboxylase activity and putrescine synthesis in arterial smooth muscle cells stimulated with platelet-derived growth factor. Exp Cell Res 1987;170:160-9.

[20] Bevers LM, Braam B, Post JA, et al. Tetrahydrobiopterin, but not L-arginine, decreases NO synthase uncoupling in cells expressing high levels of endothelial NO synthase. Hypertension 2006;47:87-94.

[21] Holm A, Baldetorp B, Olde B, Leeb-Lundberg LM, Nilsson BO. The GPER1 agonist G-1 attenuates endothelial cell proliferation by inhibiting DNA synthesis and accumulating cells in the S and G2 phases of the cell cycle. J Vasc Res 2011;48:327-35.

[22] Schwartz EL. Antivascular actions of microtubule-binding drugs. Clin Cancer Res 2009;15:2594-601.

[23] Kim S, Kawamura M, Wanibuchi H, et al. Angiotensin II type 1 receptor blockade inhibits the expression of immediate-early genes and fibronectin in rat injured artery. Circulation 1995;92:88-95.

[24] Pegg AE. Recent advances in the biochemistry of polyamines in eukaryotes. Biochem J 1986;234:249-62.

[25] Pegg AE, McCann PP. Polyamine metabolism and function. Am J Physiol 1982;243:C212-21.

[26] Powazniak Y, Kempfer AC, Pereyra JC, Palomino JP, Lazzari MA. VWF and ADAMTS13 behavior in estradiol-treated HUVEC. Eur J Haematol 2011;86:140-7.

[27] Veress I, Haghighi S, Pulkka A, Pajunen A. Changes in gene expression in response to polyamine depletion indicates selective stabilization of mRNAs. Biochem J 2000;346 Pt 1:185-91.

[28] Li D, Zhang C, Song F, Lubenec I, Tian Y, Song QH. VEGF regulates FGF-2 and TGF-beta1 expression in injury endothelial cells and mediates smooth muscle cells proliferation and migration. Microvasc Res 2009;77:134-42.

[29] Forte A, Rinaldi B, Sodano L, et al. Stem cell therapy for arterial restenosis: potential parameters contributing to the success of bone marrow-derived mesenchymal stromal cells. Cardiovasc Drugs Ther 2012;26:9-21.

[30] Perez-Cano FJ, Franch A, Castellote C, Castell M. Immunomodulatory action of spermine and spermidine on NR8383 macrophage line in various culture conditions. Cell Immunol 2003;226:86-94.

[31] Bjelakovic G, Stojanovic I, Jevtovic Stoimenov T, et al. Metabolic correlations of glucocorticoids and polyamines in inflammation and apoptosis. Amino Acids 2010;39:29-43.

[32] Forte A, Della Corte A, De Feo M, Cerasuolo F, Cipollaro M. Role of myofibroblasts in vascular remodelling: focus on restenosis and aneurysm. Cardiovasc Res 2010;88:395-405.

[33] Cetrullo S, Tantini B, Facchini A, et al. A pro-survival effect of polyamine depletion on norepinephrine-mediated apoptosis in cardiac cells: role of signaling enzymes. Amino Acids 2010;

[34] Liu GY, Hung YC, Hsu PC, et al. Ornithine decarboxylase prevents tumor necrosis factor alpha-induced apoptosis by decreasing intracellular reactive oxygen species. Apoptosis 2005;10:569-81.

[35] Izbicka E, Streeper RT, Yeh IT, et al. Effects of alpha-difluoromethylornithine on markers of proliferation, invasion, and apoptosis in breast cancer. Anticancer Res 2010;30:2263-9.

[36] Bhattacharya S, Ray RM, Johnson LR. Role of polyamines in p53-dependent apoptosis of intestinal epithelial cells. Cell Signal 2009;21:509-22.

[37] Flamigni F, Stanic I, Facchini A, et al. Polyamine biosynthesis as a target to inhibit apoptosis of non-tumoral cells. Amino Acids 2007;33:197-202.

[38] Forte A, Galderisi U, De Feo M, et al. c-Myc antisense oligonucleotides preserve smooth muscle differentiation and reduce negative remodelling following rat carotid arteriotomy. J Vasc Res 2005;42:214-25.

[39] Forte A, Esposito S, De Feo M, et al. Stenosis progression after surgical injury in Milan hypertensive rat carotid arteries. Cardiovasc Res 2003;60:654-63.

[40] Bennett MR, Anglin S, McEwan JR, Jagoe R, Newby AC, Evan GI. Inhibition of vascular smooth muscle cell proliferation in vitro and in vivo by c-myc antisense oligodeoxynucleotides. J Clin Invest 1994;93:820-8.

[41] Ji R, Cheng Y, Yue J, et al. MicroRNA expression signature and antisense-mediated depletion reveal an essential role of MicroRNA in vascular neointimal lesion formation. Circ Res 2007;100:1579-88.

[42] Yang J, Zeng Y, Li Y, et al. Intravascular site-specific delivery of a therapeutic antisense for the inhibition of restenosis. Eur J Pharm Sci 2008;35:427-34.

[43] Durante W, Liao L, Peyton KJ, Schafer AI. Thrombin stimulates vascular smooth muscle cell polyamine synthesis by inducing cationic amino acid transporter and ornithine decarboxylase gene expression. Circ Res 1998;83:217-23.

[44] Ignarro LJ, Buga GM, Wei LH, Bauer PM, Wu G, del Soldato P. Role of the arginine-nitric oxide pathway in the regulation of vascular smooth muscle cell proliferation. Proc Natl Acad Sci U S A 2001;98:4202-8.

[45] Grove J, Fozard JR, Mamont PS. Assay of alpha-difluoromethylornithine in body fluids and tissues by automatic amino-acid analysis. J Chromatogr 1981;223:409-16.

[46] Casero RA, Jr., Marton LJ. Targeting polyamine metabolism and function in cancer and other hyperproliferative diseases. Nat Rev Drug Discov 2007;6:373-90.

[47] Heby O. Ornithine decarboxylase as target of chemotherapy. Adv Enzyme Regul 1985;24:103-24.

[48] Tulis DA, Durante W, Peyton KJ, Chapman GB, Evans AJ, Schafer AI. YC-1, a benzyl indazole derivative, stimulates vascular cGMP and inhibits neointima formation. Biochem Biophys Res Commun 2000;279:646-52.

[49] Abe T, Sasaki M, Nakajima H, et al. [Evaluation of pluronic F127 as a base for gradual release of anticancer drug]. Gan To Kagaku Ryoho 1990;17:1546-50.

[50] Moore T, Croy S, Mallapragada S, Pandit N. Experimental investigation and mathematical modeling of Pluronic F127 gel dissolution: drug release in stirred systems. J Control Release 2000;67:191-202.

[51] Coats AJ, Shewan LG. Statement on authorship and publishing ethics in the international journal of cardiology. Int J Cardiol 2010;153:239-40.

Figure legends

Fig. 1. A, B: Immunohistochemical expression analysis of SM22α (A) and α-SMA (B) in primary rat carotid SMCs at passage 3 through laser-scanning confocal microscopy. C, D: Cell counting in bEnd.3 ECs (C) and primary SMCs (D) at 3 and 8 days of treatment with or without 5 mM DFMO. E: Evaluation of DNA synthesis in bEnd.3 ECs and primary SMCs at 3 and 8 days of treatment with or without 5 mM DFMO. F: FACS analysis of cell cycle distribution of bEnd.3 ECs and primary SMCs at 3 days of treatment with or without 5 mM DFMO. G-I: Immunohistochemical expression analysis of α-tubulin in bEnd.3 ECs treated with 1 and 5 mM DFMO and in control cells. Bars represent 5 μm. L: RT-PCR analysis of the expression of cyclins B1, D1 and E1 in bEnd.3 ECs and in primary SMCs at 3 days of treatment with or without 5 mM DFMO (n=3 for each group, for each time point). All data are presented as the mean ± SEM. *: $p<0.05$ vs. control cells. #: $p=0.05$ vs. control cells.

Fig. 2: RT-PCR analysis of gene expression in carotids harvested 3 hrs and 3 days after arteriotomy and perivascularly treated with 5 mg/mL DFMO or control 20% pluronic gel. Data are presented as the mean ± SEM. *: $p<0.05$ vs. pluronic gel-treated carotids.

Fig. 3: Immunohistochemical expression analysis of SM22α and vWF through laser-scanning confocal microscopy in rat carotids harvested 3 days after arteriotomy and perivascularly treated with 5 mg/mL DFMO or control 20% pluronic gel. Nuclei were counterstained with Sytox Green. Bars in A and B represent 100 μm and in D and E represent 25 μm.

Fig. 4: RT-PCR analysis of genes belonging to polyamine pathway in bEnd.3 ECs and in primary SMCs at 3 days of treatment with or without 5mM DFMO (A) (n=3 for each group) and in carotids submitted to arteriotomy and to 5 mg/ml DFMO or control 20% pluronic gel perivascular treatment and harvested 3 hrs and 3 days after injury (B) (n=5 DFMO-treated rats and n=5 pluronic gel-

treated rats, for each time point, n=4 uninjured rat carotids). Data are presented as the mean ± SEM. *: $p<0.05$ vs. control cells or vs. pluronic gel-treated carotids at the same time point.

Fig. 5: A-E: Immunohistochemical staining of BrdU in injured rat carotids at 3 days after arteriotomy and DFMO (A, B) or pluronic gel (C, D) perivascular application. Black arrows in A and C indicate the arteriotomy site. Representative BrdU-positive cells (stained in brown) are indicated by arrow heads. Hematoxylin nuclei counterstaining in blue. A, C: 40x magnification; B, D: 100x magnification of the area enclosed in the black perimeter in A and C. E: percentage in the tunicae media and intima of BrdU-positive cells (n=8 for each group). Data are presented as the mean ± SEM. *: $p<0.05$ vs. pluronic gel-treated carotids.

F-I: Immunohistochemical analysis of the apoptosis index (F, G) at 3 after carotid arteriotomy and DFMO perivascular application. Arrow heads indicate representative nuclei positive to TUNEL assay. Hematoxylin nuclei counterstaining in blue (n=8 for each group). F: 40x magnification; G: 100x magnification of the area enclosed in black perimeter in F.

H: RT-PCR analysis of mRNAs coding for Bcl-2 and Bax at 3 days after carotid arteriotomy and DFMO or control pluronic gel application and in carotids from uninjured rats (n=5 DFMO-treated rats and n=5 pluronic gel-treated rats, for each time point, n=4 uninjured rat carotids). Data are presented as the mean ± SEM. *:$p<0.05$ vs. pluronic gel-treated carotids.

I: percentage in the tunicae media and intima of TUNEL assay-positive cells at 3 days after carotid arteriotomy and DFMO perivascular application or control pluronic gel and in carotids from uninjured rats (n=8 for each group).

Fig. 6: Morphological analysis of rat carotids at 28 days after arteriotomy and DFMO (B) or pluronic gel (C) perivascular application and of uninjured carotids (A). Hematoxylin staining, bar represents 20 μm. Arrows indicate the injury site. D: Morphometric analysis of the lumen CSA in

carotids at 3, 7 and 28 days after arteriotomy and in uninjured carotids (n=5 at 3 days after arteriotomy for each group; n=5 at 7 days after arteriotomy, for each group; n=10 at 28 days after arteriotomy, for each group). Data are presented as the mean ± SEM. *:$p<0.05$ vs.carotids from uninjured rats. [§]:$p<0.05$ vs. pluronic gel-treated carotids and vs. carotids from uninjured rats.

Supplemental Figures

Supplemental figure 1: ELISA analysis of rat serum samples harvested at 3 hrs and 3 days after arteriotomy and DFMO or control pluronic gel treatment and of serum from uninjured rats (n=5 for each group, for each time point). Data are presented as the mean ± SEM. *:$p<0.05$ vs. pluronic gel-treated carotids.

Fig.1

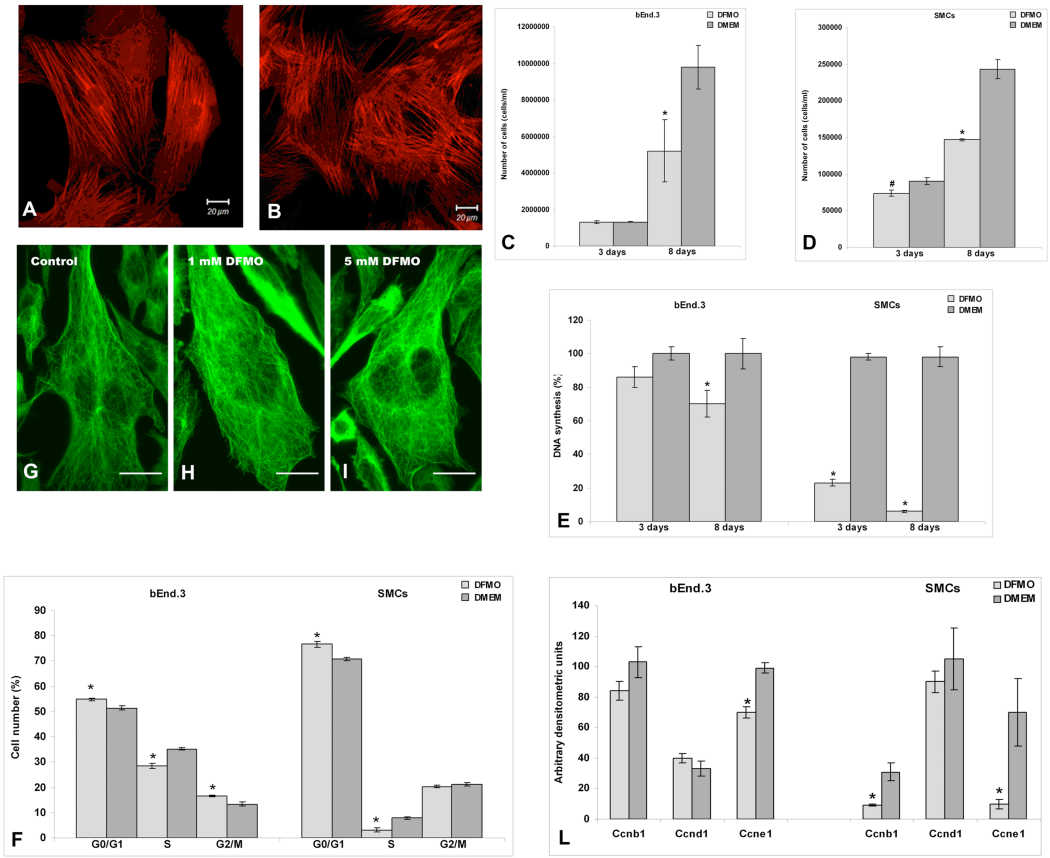
A
20 μm
B
20 μm
bEnd.3
DFMO
DMEM
Number of cells (cells/ml)
12000000
10000000
8000000
6000000
4000000
2000000
0
3 days
8 days
C
SMCs
DFMO
DMEM
Number of cells (cells/ml)
300000
250000
200000
150000
100000
50000
0
3 days
8 days
D
Control
1 mM DFMO
5 mM DFMO
G
H
I
bEnd.3
SMCs
DFMO
DMEM
DNA synthesis (%)
120
100
80
60
40
20
0
3 days
8 days
3 days
8 days
E
bEnd.3
SMCs
DFMO
DMEM
Cell number (%)
90
80
70
60
50
40
30
20
10
0
G0/G1
S
G2/M
G0/G1
S
G2/M
F
bEnd.3
SMCs
DFMO
DMEM
Arbitrary densitometric units
140
120
100
80
60
40
20
0
Ccnb1
Ccnd1
Ccne1
Ccnb1
Ccnd1
Ccne1
L

Fig.2

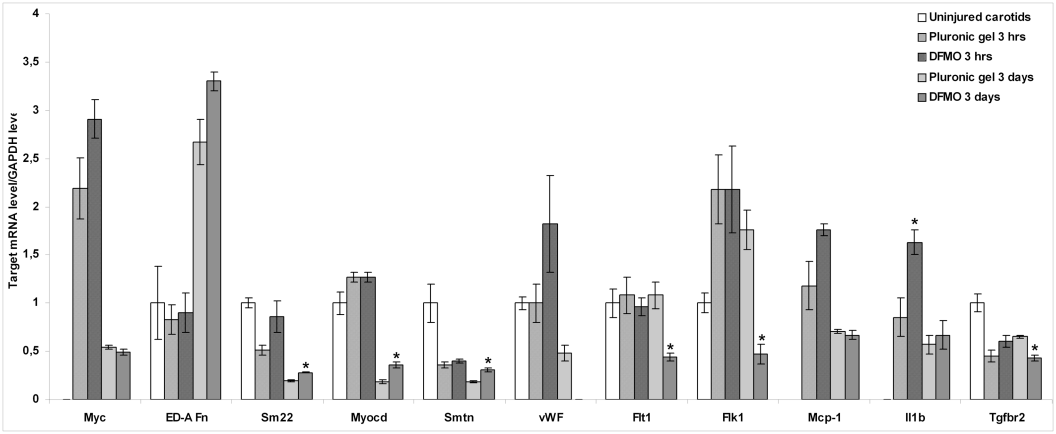
Uninjured carotids
Pluronic gel 3 hrs
DFMO 3 hrs
Pluronic gel 3 days
DFMO 3 days
Target mRNA level/GAPDH level
4
3,5
3
2,5
2
1,5
1
0,5
0
Myc
ED-A Fn
Sm22
Myocd
Smtn
vWF
Flt1
Flk1
Mcp-1
Il1b
Tgfbr2
*

Fig.3

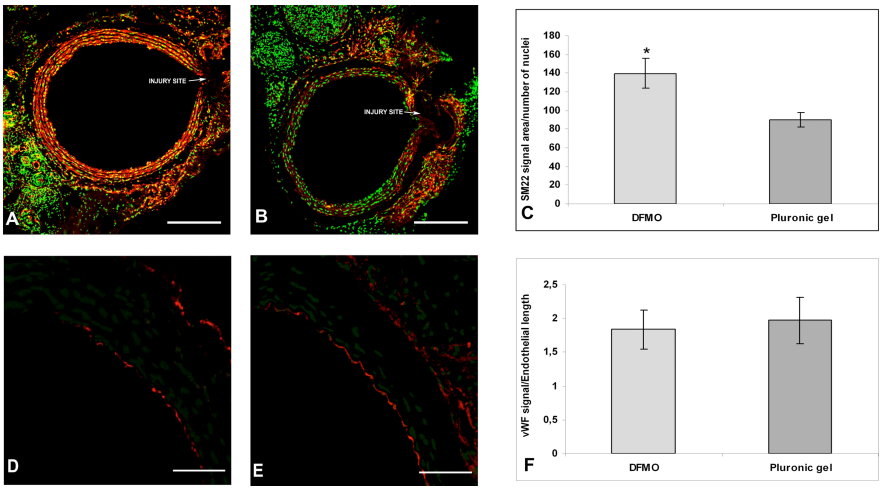
INJURY SITE
A
INJURY SITE
B
SM22 signal area/number of nuclei
180
160
140
120
100
80
60
40
20
0
*
DFMO
Pluronic gel
C
D
E
vWF signal/Endothelial length
2,5
2
1,5
1
0,5
0
DFMO
Pluronic gel
F

Fig.4

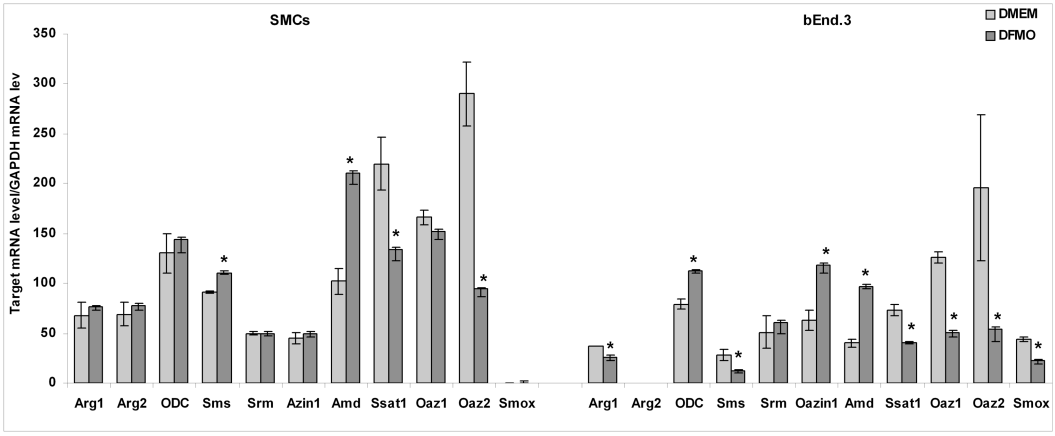
SMCs
bEnd.3
DMEM
DFMO
Target mRNA level/GAPDH mRNA lev
350
300
250
200
150
100
50
0
Arg1
Arg2
ODC
Sms
Srm
Azin1
Amd
Ssat1
Oaz1
Oaz2
Smox
Arg1
Arg2
ODC
Sms
Srm
Oazin1
Amd
Ssat1
Oaz1
Oaz2
Smox

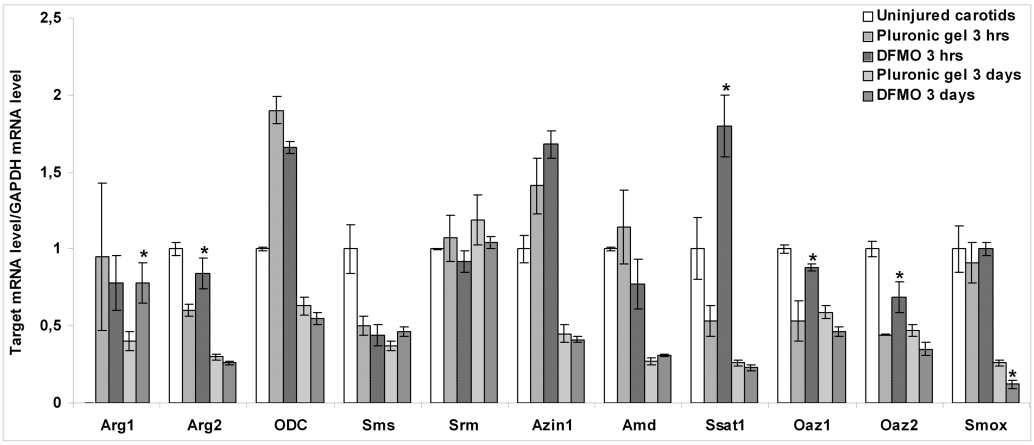
Uninjured carotids
Pluronic gel 3 hrs
DFMO 3 hrs
Pluronic gel 3 days
DFMO 3 days
Target mRNA level/GAPDH mRNA level
2,5
2
1,5
1
0,5
0
Arg1
Arg2
ODC
Sms
Srm
Azin1
Amd
Ssat1
Oaz1
Oaz2
Smox

Fig.5

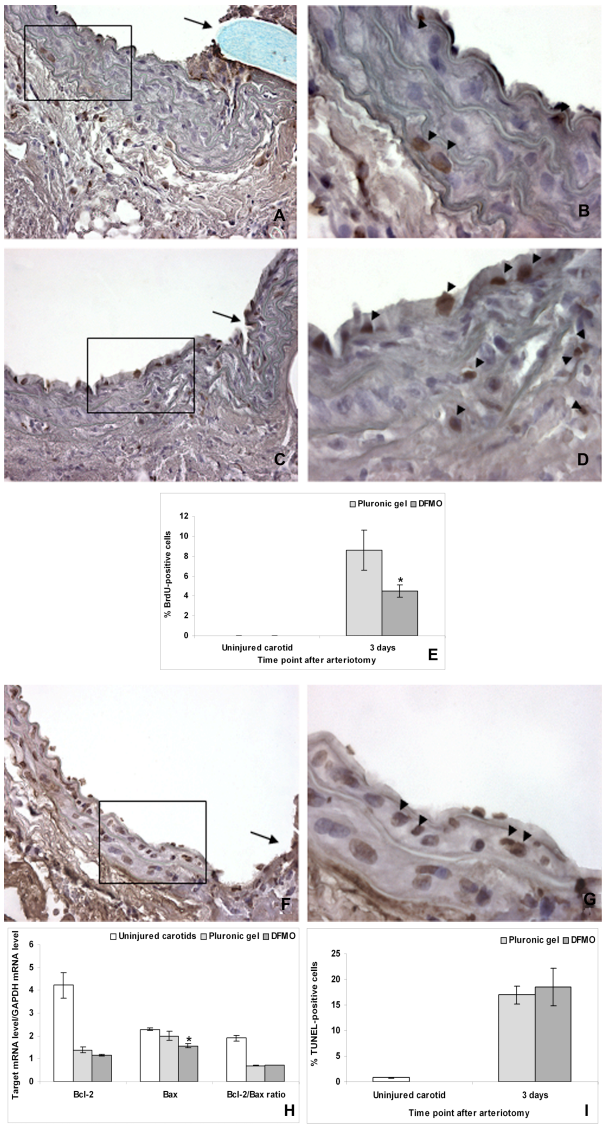
A
B
C
D
Pluronic gel
DFMO
% BrdU-positive cells
12
10
8
6
4
2
0
*
Uninjured carotid
3 days
Time point after arteriotomy
E
F
G
Uninjured carotids
Pluronic gel
DFMO
Target mRNA level/GAPDH mRNA level
6
5
4
3
2
1
0
*
Bcl-2
Bax
Bcl-2/Bax ratio
H
Pluronic gel
DFMO
% TUNEL-positive cells
25
20
15
10
5
0
Uninjured carotid
3 days
Time point after arteriotomy
I

Fig.6

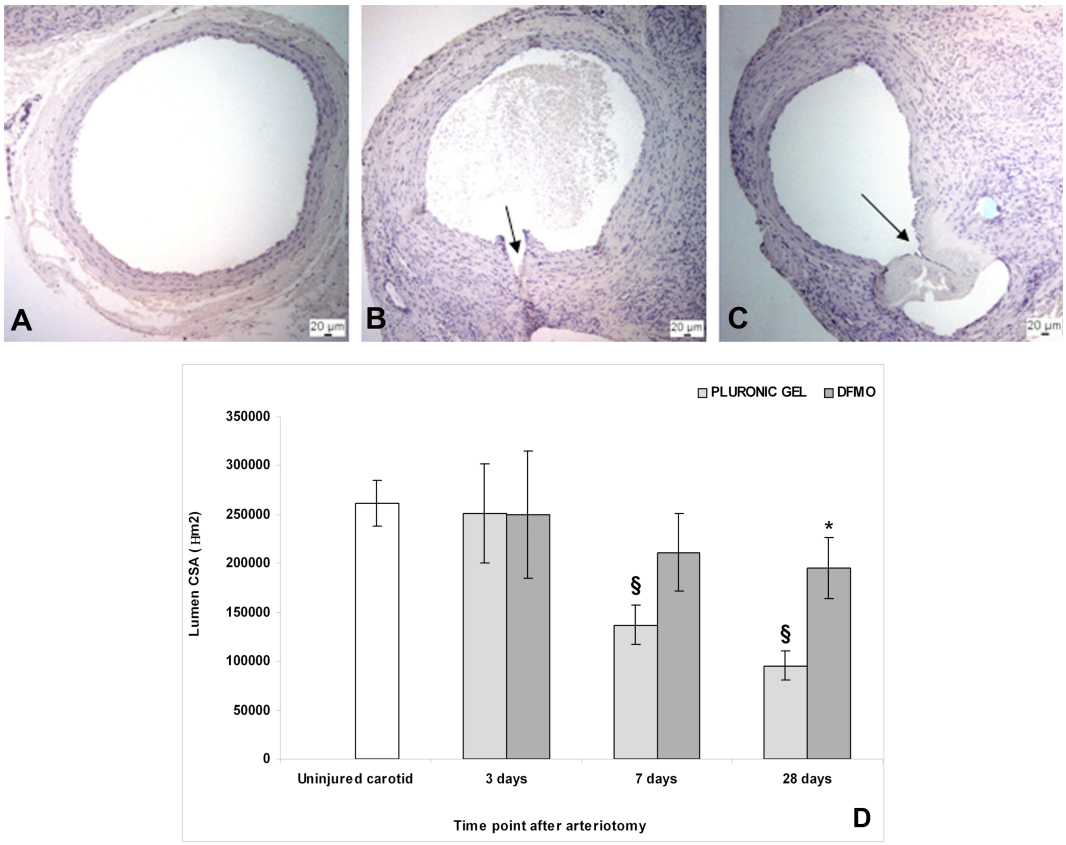
A
20 µm
B
20 µm
C
20 µm
PLURONIC GEL
DFMO
Lumen CSA (µm2)
350000
300000
250000
200000
150000
100000
50000
0
§
§
*
Uninjured carotid
3 days
7 days
28 days
Time point after arteriotomy
D

Supplement fig.1

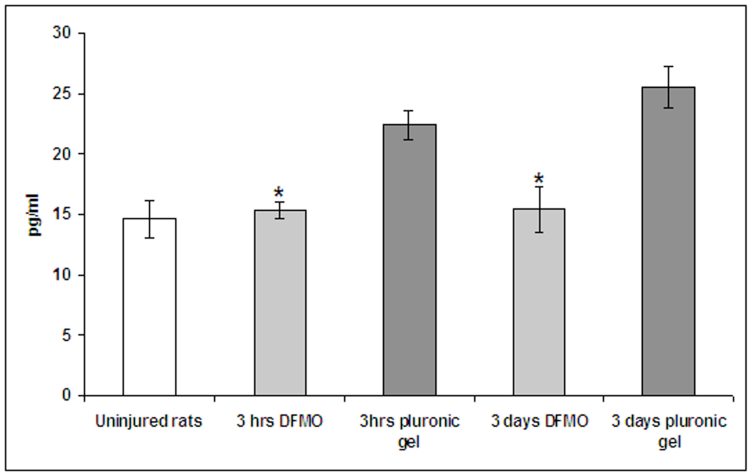

Supplemental Table 1: Summary of the PCR primer sequences and annealing temperatures for each target gene analysed in rat and mice carotid samples and cultured cells.

Species	Target gene	Primer sequence	ANNEALING T (°C)
Rat	Odc	5'-TTTTGCGGATTGCCACTGA-3' 5'-GCTCTTTTGCCCGTTCCAA-3'	59
	Srm	5'-TGCGAGATCGATGAGGATGTC-3' 5'-AACTCAAAGCCATCGCCCA-3'	60
	Sms	5'-TTTGAAAGTCAGCCGGAGGA-3' 5'-AAACCCAAACCCCACACAGAG-3'	57
	Amd	5'-TGGTCTTTCACCATGGCGTT-3' 5'-ACCGTGCCTGTTTCTCCATTC-3'	61
	Azin1	5'-TGTTTCCGTTTCTCTCCCTGG-3' 5'-CGGCGCGAGAAAAAGAAGA-3'	61
	Arg1	5'-TCCAAGCCAAAGCCCATAGA-3' 5'-TTTAAGCTTCTCCACCAGGCC-3'	60
	Arg2	5'-TCCT CATTTGGCCACTTCTGA-3' 5'-CAATGTGTCCGCCTTCTCTTG-3'	59
	Ssat1	5'-TGCTATGAAGTGTCGCTGCAG-3' 5'-TTCACTGGACAGATCCGAAGC-3'	57
	Smox	5'-TGCAGAGCGTGAAACTTGGA-3' 5'-AGGCCATTGGCTTCTGCTAGT-3'	60
	Oaz1	5'-AGCGGAGGTTTTTGCTGGTT-3' 5'-CCCTTCTTTCTCTCTGGCGAA-3'	62
	Oaz2	5'-TTCCGGCATTTTGTGTCTGG-3' 5'-GCCCCTATGTAAAATGCACGG-3'	58
	SM22α	5'- AGGATTATGGAGTCACGAAGA -3' 5'- GATGGGGGAAACGGTAGAGGT -3'	54
	Myocardin	5'- GTGCATATTAACCAGGCTGGC -3' 5'- GTTCCATGACCCGAGGAAA -3'	59
	Smoothelin	5'- AAACTAACACGAAATCGCGCC -3' 5'- AAGGCCTCATCTGCCATCTTG -3'	61
	vWF	5'- TCAAGAAGAAGAAGGTCATT -3' 5'- CAAGGTCGCAGAGGTAGTTA -3'	52.2
	VEGF	5'- GCCGTCCTGTGTGCCCCTAATG -3' 5'- GTTCTATCTTTCTTTGGTCTGC -3'	54.3

	Flt-1	5’- AAAAGATACCAACCGAAGGAGA -3’ 5’- TAGAAGGAGCCAAAAGAGTGTC -3’	55.5
	Flk-1	5’- GAGGGACCTGGATTGGCTTTGG -3’ 5’- CTTCTTATGCTGATGCTTTGA -3’	54.6
	Tgfb1	5’- TGCTAATGGTGGACCGCAA -3’ 5’- CACTGCTTCCCGAATGTCTGA -3’	57
	Tgfbr1	5’- CATCGGCAAAGGTCGGTTT -3’ 5’- CCTCTCGGAACCATGAACGTT -3’	59
	Tgfbr2	5’- CAGCTGTGCAAGTTTTGCGAC 3’ 5’- TTCCTGCGGCTTCTCACAGAT 3’	60
	Trpc1	5’- ACCTGCTTTGCTCTGTTCTGG - 3’ 5’-GCCGTCTGACCTTGCCTTTGG - 3’	57
	Trpc6	5’- CAGAATGCAGCCAGAAACAAA - 3’ 5’- ACAGCGAGGACCACGAGGAAT – 3’	56
	Mcp 1	5’- CAGATGCAGTTAATGCCCCA -3’ 5’- CCTGCTGCTGGTGATTCTCTT -3’	59
	IL-1 β	5’- TATGTCTTGCCCGTGGAGCTT -3’ 5’- TAGCAGGTCGTCATCATCCCA -3’	54.6
	GAPDH	5’- GCATCCTGCACCAACTG -3’ 5’- GCCTGCTTCACCACCTTCTT -3’	57
	Ccnb1	5’-TGCTGCAGGAGACCATGTACA-3’ 5’-TGGCAGTTACACCAACCAGCT-3’	59
	Ccnd1	5’-TGCTTCTGGTGAACAAGCTCA-3’ 5’-ATCTGCTTGTTCTCATCCGCC-3’	59
	Ccne1	5’-GTGGCCGTTTTTTTGCAAGA-3’ 5’-TCCACGCACGCTGAATCAT-3’	58
	Odc	5’-GACCCAAGCCAGACGAGAAGTA-3’ 5’- CATGCATTTCAGGCAGGTTACA-3’	60
	Srm	5’-GGTCCAGTGCGAGATTGATGA-3’ 5’-AACTCAAAGCCATCGCCCA-3’	60
	Sms	5’-TCTCCGTTTTGAGCCCTTGTT-3’ 5’-AAGAGGCAGCCAAAGCGAA-3’	60
	Amd	5’-TGAGGTCTGATTTCCCCGTCT-3’ 5’-CACCAAAACTTCCCCACCTGT-3’	56
	Azin1	5’-CCTTTGTAGCAGGTGTGGACCA-3’ 5’-TCAGCCGTATTCCACAAAGCC-3’	59
Mice	Arg1	5’-AACACGGCAGTGGCTTTAA CC-3’ 5’-GGTTTTCATGTGGCGCATTC-3’	59

Arg2	5’-GTTGATGCTCATGCGGACATT-3’ 5’-CCAGGAAAATCCTGGCAGTTG-3’	57
Ssat1	5’-TCCCCGAAGTAAGTTTGCCA-3’ 5’-TTCCTCATTCGTTTCCCGG-3’	60
Smox	5’-GGAGTTCTTCCGGCATGGTAA-3’ 5’-TGGATCATGGCGAGCTTCA-3’	62
Oaz1	5’-ATGGTGAAATCCTCCCTGCAG-3’ 5’-TGACTAAGAAGCGGCATGGTG-3’	62
Oaz2	5’-CAGAGCCACCGAGGATGATAA-3’ 5’-ACAGAGGCCCTGGAACAATGT-3’	60
Ccnb1	5’-TGGCCTCACAAAGCACATGA-3’ 5’-ATGCCTTTGTCACGGCCTTAG-3’	58
Ccnd1	5’-TGCTGCAAATGGAACTGCTTC-3’ 5’-CATCCGCCTCTGGCATTTT-3’	60
Ccne1	5’-TGTTACAGATGGCGCTTGCTC-3’ 5’-TTCAGCCAGGACACAATGGTC-3’	59
GAPDH	5’- GCATCCTGCACCAACTG -3’ 5’- GCCTGCTTCACCACCTTCTT -3’	57

Supplemental Table 2: Treatment with 1 mM DFMO for 3 days reduces polyamine levels in primary rat carotid SMCs and endothelial bEnd.3 cells. The polyamines, i.e. putrescine, spermidine and spermine, were determined in cell homogenates by HPLC. Values are means ± SEM of 5 observations in each group. * represents P<0.001.

	Putrescine (nmol/mg protein)		**Spermidine (nmol/mg protein)**		**Spermine (nmol/mg protein)**	
	Control	**DFMO**	**Control**	**DFMO**	**Control**	**DFMO**
Rat carotid VSMCs	2.93±2.23	0±0*	13.7±1.8	1.7±1.6*	50.3±14.7	39.2±5.5
bEnd.3 ECs	1.58±0.28	0±0*	27.9±1.8	7.8±0.4*	23.7±1.3	24.4±1.7